

A Journal of the Gesellschaft Deutscher Chemiker

# Angewandte Chemie

GDCh

International Edition

[www.angewandte.org](http://www.angewandte.org)

## Accepted Article

**Title:** Synthesis and Optoelectronic Applications of  $d\pi$ - $\pi\pi$  Conjugated Polymers with a Di-metallaaromatic Acceptor

**Authors:** Shiyang Chen, Lingwei Feng, Lixia Peng, Xiang Gao, Yongfa Zhu, Liulin Yang, Dafa Chen, Kai Zhang, Xugang Guo, Fei Huang, and Haiping Xia

This manuscript has been accepted after peer review and appears as an Accepted Article online prior to editing, proofing, and formal publication of the final Version of Record (VoR). The VoR will be published online in Early View as soon as possible and may be different to this Accepted Article as a result of editing. Readers should obtain the VoR from the journal website shown below when it is published to ensure accuracy of information. The authors are responsible for the content of this Accepted Article.

**To be cited as:** *Angew. Chem. Int. Ed.* **2023**, e202305489

**Link to VoR:** <https://doi.org/10.1002/anie.202305489>

# Synthesis and Optoelectronic Applications of $d_{\pi}$ - $p_{\pi}$ Conjugated Polymers with a Di-metallaaromatic Acceptor

Shiyan Chen<sup>+, [a]</sup> Lingwei Feng<sup>+, [b]</sup> Lixia Peng,<sup>[c]</sup> Xiang Gao,<sup>[c]</sup> Yongfa Zhu,<sup>[c]</sup> Liulin Yang,<sup>[c]</sup> Dafa Chen,<sup>[a]</sup> Kai Zhang,<sup>\*, [b]</sup> Xugang Guo,<sup>[d]</sup> Fei Huang,<sup>[b]</sup> and Haiping Xia<sup>\*, [a]</sup>

[a] Dr. S. Chen, Prof. D. Chen, Prof. H. Xia

Shenzhen Grubbs Institute and Department of Chemistry

Southern University of Science and Technology

Shenzhen 518055, China

E-mail: [xiahp@sustech.edu.cn](mailto:xiahp@sustech.edu.cn)

[b] L. Feng, Prof. K. Zhang, Prof. F. Huang

Institute of Polymer Optoelectronic Materials and Devices, State Key Laboratory of Luminescent Materials and Devices

South China University of Technology

Guangzhou 510640, China.

E-mail: [mszhangk@scut.edu.cn](mailto:mszhangk@scut.edu.cn)

[c] L. Peng, X. Gao, Y. Zhu, Dr. L. Yang

State Key Laboratory of Physical Chemistry of Solid Surfaces and Collaborative Innovation Center of Chemistry for Energy Materials (iChEM), College of

Chemistry and Chemical Engineering

Xiamen University

Xiamen 361005, China.

[d] Prof. X. Guo

Department of Materials Science and Engineering

South China University of Technology

Shenzhen 518055, China.

[+] These authors contributed equally to this work.

Supporting information for this article is given via a link at the end of the document.

**Abstract:** The development of conjugated polymers especially n-type polymer semiconductors is powered by the design and synthesis of electron-deficient building blocks. Herein, a strong acceptor building block with di-metallaaromatic structure was designed and synthesized by connecting two electron-deficient metallaaromatic units through a  $\pi$ -conjugated bridge. Then, a double-monomer polymerization methodology was developed for inserting it into conjugated polymer scaffolds to yield metallopolymers. The isolated well-defined model oligomers indicated polymer structures. Kinetic studies based on nuclear magnetic resonance and ultraviolet-visible spectroscopies shed light on the polymerization process. Interestingly, the resulted metallopolymers with  $d_{\pi}$ - $p_{\pi}$  conjugations are very promising electron transport layer materials which can boost photovoltaic performance of an organic solar cell, with power conversion efficiency up to 18.28% based on the PM6:EH-HD-4F non-fullerene system. This work not only provides a facile route to construct metallaaromatic conjugated polymers with various functional groups, but also discovers their potential applications for the first time.

## Introduction

The wide applications of conjugated polymers have attracted much attention.<sup>[1,2]</sup> Among them, p-type (hole transporting) polymer semiconductors have developed quickly and reached a remarkable advance.<sup>[3]</sup> In a sharp contrast, the development of n-type (electron transporting) polymers lags far behind, although

they are essential for realizing organic complementary logic circuits and p-n junction devices.<sup>[4,5]</sup> For example, n-type polymer semiconductors are widely used as active layer or electron-transporting materials in organic photovoltaics.<sup>[2c,6]</sup> One of the factors limiting the development of n-type polymers is the lack of suitable acceptor building blocks, which are essential for such kind of materials. An ideal acceptor building block should have characteristics of electron-deficiency, suitable energy level, excellent solubility, and highly planar framework.<sup>[7,8]</sup> At present, acceptor building blocks that meet these conditions and can construct high-performance n-type polymer semiconductors are scarce and usually involve one of the four strong electron-withdrawing groups (EWGs) including imide, amide, B←N, and CN groups (Figure 1a).<sup>[4b,9]</sup> Therefore, it is of great significance to design and synthesize novel acceptor building blocks owing to their critical role in the development of n-type polymer semiconductors and even the whole conjugated polymers.

Donor-acceptor (D-A) type polymers are one of the fundamental configurations of n-type polymer semiconductors.<sup>[10]</sup> Owing to the strong intramolecular charge transfer (ICT) caused by the electron push-pull effect between electron-donating unit and electron-withdrawing unit (D-A effect), the optical bandgap of polymers could be further narrowed.<sup>[11,12]</sup> In addition, the energy level of conjugated polymers could be easily tuned through the suitable chosen of donor and acceptor units. However, as mentioned above, development of new acceptor building blocks remains great challenge.

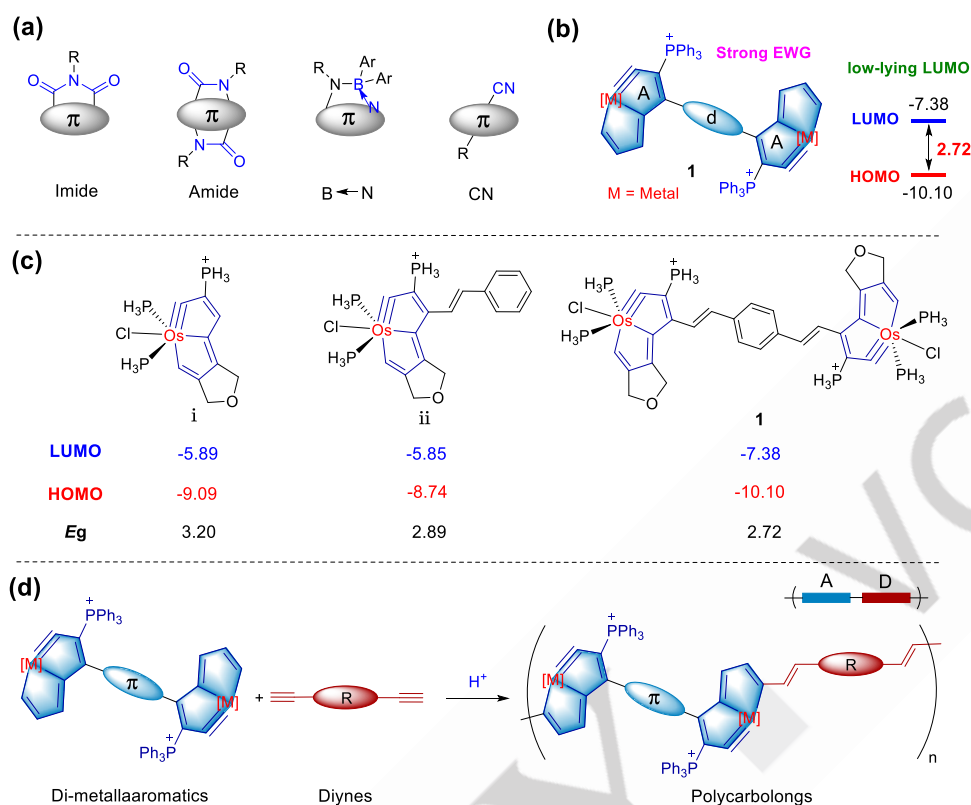


**Figure 1.** Design of monomers and polymers. (a) Four typical strong electron-withdrawing groups (EWGs) for n-type polymers. (b) Structure of Acceptor-donor-Acceptor (A-d-A) type di-metallaaromatic building block and corresponding molecular engineering strategies (this work). (c) The HOMO and LUMO energy levels of mono-metallaaromatic and di-metallaaromatic units as a comparison. The frontier molecular orbital levels are calculated via density functional theory (DFT) at the B3LYP/6-31G (d) level (SDD for Os), and are given in kcal mol<sup>-1</sup>. (d) A<sub>2</sub> + B<sub>2</sub> type double-monomer polymerization route toward polycarbolongs.

Recently, we reported a novel kind of  $d_{\pi}$ - $\pi_{\pi}$  conjugated polymers (namely polycarbolongs) based on a mono-metallaaromatic framework **i** via AB-type single-monomer metal carbyne shuttling polymerization.<sup>[13]</sup> The building block **i** with electron-deficient characteristics is a potential acceptor unit, reflected by the low calculated lowest unoccupied molecular orbital (LUMO) as -5.89 eV. We aimed to further enhance the electron-deficient characteristic by lowering the LUMO value. To achieve this, herein, two electron-deficient metallaaromatic units were connected through a  $\pi$ -conjugated bridge, leading to a di-metallaaromatic unit **1**, which is in an acceptor-donor-acceptor (A-d-A) type configuration (Figure 1b). The calculated LUMO of **1** could reach -7.38 eV, which is about 1.50 eV lower than those of the mono-metallaaromatic unit **i** and a similar mono-metallaaromatic model **ii** (Figure 1c or Figure S1). To introduce it into conjugated polymers, a A<sub>2</sub> + B<sub>2</sub> type double-monomer metal carbyne shuttling polymerization was developed, and in this methodology, the other monomer is diynes that allow for the introduction of different frameworks and functional groups easily (Figure 1d). The obtained D-A alternative conjugated polymers have n-type semiconductor characteristics, and they show good solubility, diverse structures, and tunable properties. Moreover, they are very promising candidates as electron transport layer

materials in organic solar cells, which can boost the photovoltaic performance of a device, with power conversion efficiency up to 18.28% based on the PM6:EH-HD-4F non-fullerene system.

## Results and Discussion

### Preparation of A Di-metallaaromatic Acceptor.

A series of di-metallaaromatic monomers (**1a-1c**) were synthesized by the treatment of multiyne carbon chains (**L1a-L1c**) with OsCl<sub>2</sub>(PPh<sub>3</sub>)<sub>3</sub> and PPh<sub>3</sub> in dichloromethane (DCM) at room temperature (RT) (see Supporting Information (SI) for details). As shown in Figure 2, the metallacyclic units are connected by different  $\pi$ -conjugated bridges. All the di-metallaaromatic monomers were characterized by nuclear magnetic resonance (NMR) spectroscopy, elemental analysis (EA) and high-resolution mass spectrometry (HRMS) (Figures S2-S31). The structures of **1a** and **1c** were confirmed by X-ray crystallography (Figure 2 or Figures S32 and S33).<sup>[14]</sup> The terminal diynes used in this work were commercially available or could be readily synthesized using published methods (Figures S38-S53).

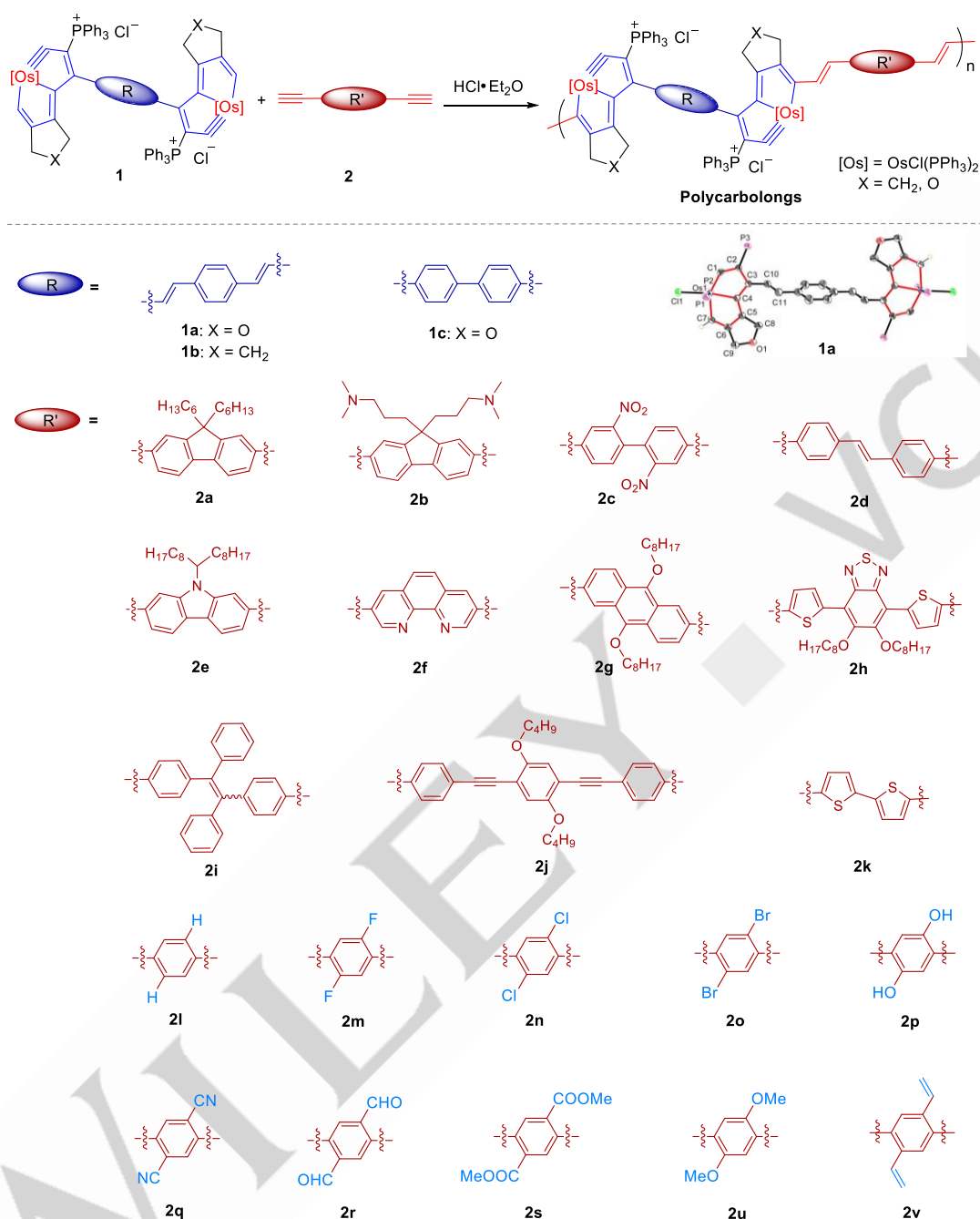


**Figure 2.** Schematic illustration of the polymerization route. Polymerization of di-metallaaromatic complexes and diynes. Insert: The X-ray molecular structure for the cation of complex 1a. Ellipsoids are at the 50% probability level; phenyl groups in PPh<sub>3</sub> are omitted for clarity.

The π-conjugated bridges 1,4-divinylphenyl and biphenyl are usually regarded as donor units,<sup>[10a]</sup> and the electron-deficient metallaaromatic frameworks on both sides act as acceptor units. Therefore, the di-metallaaromatics are in an A-d-A type configuration (Figure 1b), just like the famous non-fullerene acceptors ITIC.<sup>[2c]</sup> Noteworthy, unlike common organic acceptors that long alkyl or alkoxy side chains are usually needed to improve their solubility, no such chains are necessary for the di-metallaaromatic unit 1. This is due to not only the bulky ligands on the metal weakening π-π stacking of molecules, but also its cationic nature. Benefit from the advanced design of A-d-A type configuration, the di-metallaaromatics is more electron-

deficient than that of mono-metallaaromatic unit, reflected by the calculated and experimental lower LUMO energy levels, as also discussed in the introduction, enabling them as promising electron-deficient building blocks for constructing n-type polymer semiconductors (Figure 1c, Figures S34-S36, and Table S2).

In an effort to understand the essential reason for acceptor characteristics, we performed DFT calculations. The structure of 1a-H, which has hydrogen atoms replacing the charged triphenylphosphonium substituents in 1a, shows a higher LUMO energy level (-2.31 eV, Figure S37). It suggests that the charged triphenylphosphonium substituents are the key for the acceptor nature.

### A Double-Monomer Metal Carbyne Shuttling Polymerization.

To obtain polycarbologs, different polymerization conditions were systematically optimized with a di-metallaaromatic complex (**1a**) and a diyne (**2a**) as the monomers. Various conditions including pH, solvent, temperature, concentration, reaction time and the ratios of monomers, were investigated (see SI for the optimisation details). Finally, with a monomer concentration of 20 mM in DCM, a solution in ether of HCl·Et<sub>2</sub>O as the acid, and a reaction atmosphere of nitrogen at RT were selected as the optimal conditions for the polymerization.

With these optimized conditions, different diynes and di-metallaaromatic monomers were examined to test the robustness and gality of the polymerization. The common building blocks of conjugated polymers such as fluorene (**2a** and **2b**), biphenyl (**2c**), *p*-phenylene vinylene (**2d**), carbazole (**2e**),

phenanthroline (**2f**), anthracene (**2g**), benzothiadiazole (**2h**), tetraphenylethene (**2i**), *p*-phenylene ethynylene (**2j**), thiophene (**2k**), and benzene (**2l**), all performed well in these polymerization reactions. In addition, the functional group tolerance was investigated. Common substituents, such as dimethylamino (**2b**), nitro (**2c**), alkoxy (**2j** and **2u**), halogen (**2m-2o**), hydroxyphenyl (**2p**), cyano (**2q**), formyl (**2r**), methoxycarbonyl (**2s**), and terminal alkenyl (**2v**) are all compatible with the polymerization route. The different spacer groups (**1a**, **1c**) and different substituents (**1a**, **1b**) in the di-metallaaromatic monomers do not affect the polymerization as well. As a result, a series of polycarbologs with diverse spacer groups and functional groups can be produced (Table 1). The NMR spectra and gel-permeation chromatography (GPC) provide structural details of the polycarbologs (Figures S54-S144). These results confirmed the generality of this polymerization.

**Table 1.** Various polycarbologs by polymerization of diynes and di-metallaaromatics.

Polycarbolog	Diyne	Di-metallaaromatic complex	Yield <sup>[a]</sup>	<i>M<sub>r</sub></i> / <i>M<sub>w</sub></i> (kDa) <sup>[b]</sup>	PDI <sup>[b]</sup>
P1	2a	1a	93	19.2/26.0	1.35
P2	2b	1a	90	15.3/16.8	1.10
P3	2c	1a	92	20.2/31.3	1.55
P4	2d	1a	94	26.3/45.5	1.73
P5	2d	1b	95	17.1/23.6	1.38
P6	2d	1c	96	47.9/89.7	1.87
P7	2e	1a	93	20.6/28.9	1.40
P8	2f	1a	90	14.7/17.3	1.17
P9	2g	1a	92	18.3/25.9	1.42
P10	2h	1a	91	16.1/21.2	1.32
P11	2i	1a	93	21.3/36.3	1.70
P12	2j	1a	93	21.4/37.4	1.75
P13	2k	1a	91	16.4/18.6	1.13
P14	2l	1a	94	32.1/54.5	1.70
P15	2m	1a	91	20.7/28.1	1.36
P16	2n	1a	92	20.6/28.1	1.36
P17	2o	1a	95	20.1/27.2	1.35
P18	2p	1a	90	14.7/16.3	1.11
P19	2q	1a	94	16.9/22.8	1.34
P20	2r	1a	93	17.7/24.9	1.41
P21	2s	1a	94	19.6/26.9	1.37
P22	2u	1a	91	15.4/17.3	1.12
P23	2v	1a	92	22.8/31.8	1.40

[a] Typical polymerization conditions: 20 mM di-metallaaromatic complex **1**, 20.5 mM diyne **2**, and 0.20 M HCl·Et<sub>2</sub>O were polymerized in dry DCM at RT under nitrogen for 24 h. Special instructions: the diynes **2b** and **2p** were polymerized in dry MeCN (2 mM); the diyne **2h** was polymerized in dry 1,2-dichloroethane with 0.10 M HCl·Et<sub>2</sub>O. Yields are for isolated products. [b] Molecular weight (using polystyrenes as standard) determined by gel permeation chromatography (GPC), using DMF with 1.0 g L<sup>-1</sup> LiBr salt added as the eluent. Number-average molecular weight (*M<sub>n</sub>*). Weight-average molecular weight (*M<sub>w</sub>*). Polydispersity (PDI) = *M<sub>w</sub>*/*M<sub>n</sub>*.

Adopting the double-monomer polymerization methodology exhibits obvious advantages compared to the previous AB-type single-monomer polymerization.<sup>[13]</sup> The monomer diynes are abundant, because they are often commercially available or simply synthesized through Sonogashira coupling from the dihalogen precursors. As a result, the skeletons of conjugated polymers can be easily functionalized, making it convenient to tune the basic physical properties, such as energy level, solubility and self-assembly, for the targeted polycarbologs, which might open up significant opportunities for the area of functional materials.

To gain further insight into the spatial configuration of polycarbologs, model complex **3** and oligomers **4** and **5** (Figure 3) were synthesized. The structures of these complexes were all confirmed by NMR spectroscopy, EA and HRMS (Figures S145-S156). These results again verified the polycarbolog structures. To reveal the polymerization mechanism, *in situ* <sup>31</sup>P and <sup>1</sup>H NMR spectroscopies were further performed for the reaction of the dimetallaaromatic complex (**1a**) with the diyne (**2d**) (Figures S169 and S170). The <sup>31</sup>P NMR singlets of the precursor monomer (**1a**) corresponding to CPh<sub>3</sub> and OsPPh<sub>3</sub> are at 6.09 and 2.71 ppm respectively (Figure S169a). The metal-carbon triple bond shifted immediately upon addition of HCl-Et<sub>2</sub>O, as evidenced by the new peaks at 15.07 and 7.06 ppm belonging to the activated monomer (**1a'**). Subsequently, these two new peaks significantly decreased, and two peaks at 4.75 and 0.05 ppm of the

polycarbolog (**P4**) appeared within 1 min. Ultimately, only two singlets belonging to the polycarbolog (**P4**) remained. The results revealed that the complex (**1a**) is the precursor monomer, and the metal-carbon triple bond shifted product (**1a'**) is the activated monomer. In the precursor monomer (**1a**), the metal carbyne (Os≡C) in each osmaaromatic unit is blocked by the bulky triphenylphosphonium substituents, rendering the carbynes dormant. During the polymerization process, the added acid caused the carbyne shift to an adjacent five-membered ring (**1a'**), leaving the carbyne without bulky neighbours in the active state, and highly reactive with diynes. After the polyaddition, the carbyne reverts to the initial dormant state, leading to conjugated polymers with a metal carbyne unit in the main chain. And this metal carbyne shuttling polymerization *via* A<sub>2</sub> + B<sub>2</sub> type double-monomer polymerization was similar to the previous AB-type single-monomer polymerization.<sup>[13]</sup> The corresponding mechanisms for the polymerization are shown in Figure S172. To reveal the kinetics of this polymerization, the formation of polycarbolog (**P4**) was monitored by ultraviolet–visible (UV-Vis) spectroscopy. A new absorption peak at 600 nm from **P4** was observed and increased gradually. The time dependent peak intensity and the kinetic variation of the *in situ* UV/Vis absorption spectra at 600 nm were recorded to follow the generation of **P4**, and the signal reached a stable state at about 7 minutes (Figure S169). These results show that the polymerization route is very efficient.

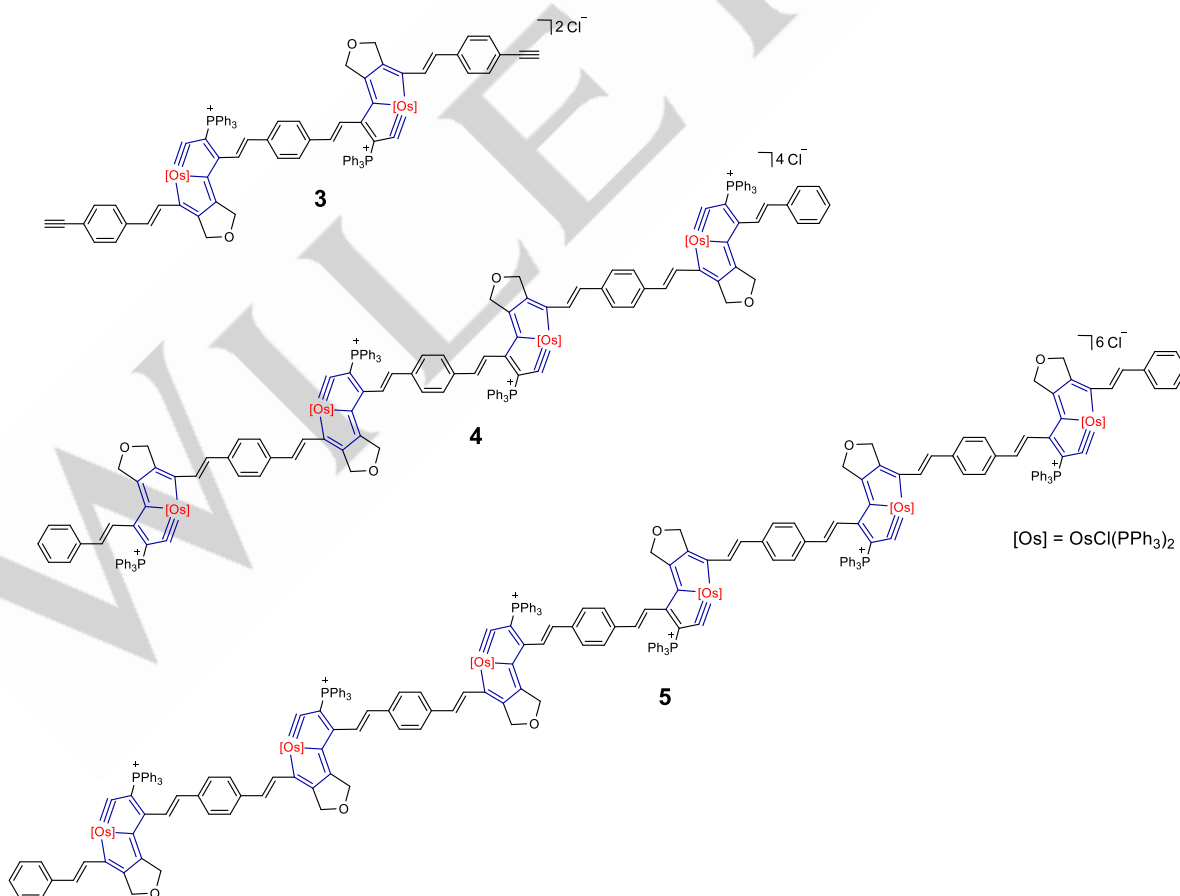
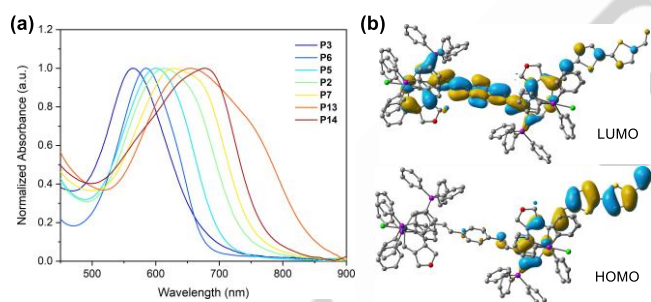


Figure 3. Molecular structures of model complex **3** and oligomers **4** and **5**.

### Physical Properties of Donor-Acceptor (D-A) Alternative Polycarbolongs.

A series of polycarbolongs prepared by current polymerization route exhibit distinct physical properties, especially the UV-Vis absorption. As shown in Figure 4a, the characteristic energy absorption bands of polycarbolongs show a  $\lambda_{\text{max}}$ , which can be varied by changing the spacer groups (see Figure S173 for the absorption spectra of all polycarbolongs). The  $\lambda_{\text{max}}$  of the polycarbolongs ranges from 565 nm (**P3**) to 678 nm (**P14**). In particular, the polycarbolong with the bithiophene spacer (**P13**) shows broad and strong absorption in the entire UV-Vis region, even extending to the near-infrared (NIR) region. Its characteristic absorption band is redshifted compared to the reported polycarbolong with the best absorption property (Figure S174).<sup>[13]</sup> The efficient ICT between the donor and acceptor may account for the outstanding absorption properties. To get more insight into the ICT interaction, the frontier molecular orbitals of the repeat unit of polycarbolong **P13** were simulated by DFT calculations (Figure 4b). The HOMO mainly delocalizes in the bithiophene, while the LUMO mainly delocalizes in the di-metallaaromatic units. These results suggest that the di-metallaaromatic unit acts as an acceptor while bithiophene acts as a donor in the polycarbolong skeletons. On the basis of absorption onsets, the optical bandgaps ( $E_g$ ) of polycarbolongs are calculated to range from 1.47 eV (**P13**) to 1.83 eV (**P6**) (Table S3).



**Figure 4.** (a) Normalized UV-Vis absorption spectra of selected polycarbolongs. (b) The frontier molecular orbitals of the repeat unit of **P13** (isovalue = 0.02).

Cyclic voltammetry (CV) measurement was performed to characterize the electrochemical properties of these polycarbolongs using ferrocene/ferrocenium ( $\text{Fc}/\text{Fc}^+$ ) redox couple as the external standard (Figures S175-S177). On the basis of their reduction onsets, the LUMOs ( $E_{\text{LUMO}}$ ) of polycarbolongs except **P8** were found to be lower than  $-3.50$  eV, indicative of their n-type characteristics (Table S3).<sup>[4b]</sup> Together, these results suggest that with such diverse absorption bands and energy levels, polycarbolongs could have extensive applications.

### Use in Organic Solar Cells (OSC).

n-Type polymer semiconductors have been widely used as electron-transporting materials in organic photovoltaics.<sup>[6]</sup> The novel  $d_{\pi}-p_{\pi}$  conjugated polycarbolongs with n-type semiconductor characteristics may exhibit unique optoelectronic

properties. Accordingly, the polycarbolongs **P1**, **P7** and **P9** were chosen as the electron transporting layer (ETL) materials in organic solar cells (OSC) and their photovoltaic performance and application potential were evaluated. The commonly used ETL material, PDINO was also adopted in control devices.<sup>[15]</sup> The device structure was defined as ITO/2PACz/PM6:EH-HD-4F/ETL (1 mg  $\text{ml}^{-1}$ )/Ag (Figure 5a),<sup>[16]</sup> and the corresponding molecular structures are shown in Figures 5b and 5c. The corresponding device performance parameters are listed in Table 2. It was observed that the control device with PDINO as ETL gave a best power conversion efficiency (PCE) of 17.62%. With devices modified with polycarbolongs, excellent photovoltaic performances were observed. Of these, **P7** gave the comparable performance as PDINO with a best PCE of 17.69%, while **P1** and **P9** gave even higher PCEs of 18.09% and 18.28%, respectively. These results show the great potential of these polycarbolongs when they are used as ETLs in OSCs. The external quantum efficiency (EQE) curves of OSCs were also measured and are presented in Figure S178b. The EQE values over 80% between 550 ~ 820 nm indicate the efficient photon to electron conversion in these devices.

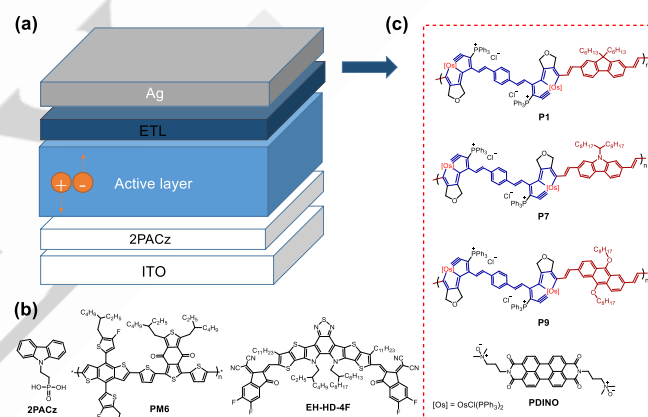


**Figure 5.** (a) Conventional structure of photovoltaic devices and chemical structures of (b) various molecules used as electron-transporting layers (ETL). (c) Chemical structures of hole-transporting layer (2PACz), donor (PM6) and acceptor (EH-HD-4F).

In order to better understand the effect of polycarbolongs on the performance of OSCs, the charge dissociation probabilities  $P(E, T)$  of these OSCs with different ETLs were assessed. The relationship of the photocurrent density ( $J_{\text{ph}}$ ) and effective voltage ( $V_{\text{eff}}$ ) of the devices were characterized and are shown in Figure S179.<sup>[17]</sup>  $J_{\text{ph}}$  is defined as  $J_{\text{ph}} = J_{\text{L}} - J_{\text{D}}$ , where  $J_{\text{L}}$  and  $J_{\text{D}}$  denote the device current density under light and dark conditions, respectively, and  $V_{\text{eff}}$  is defined as  $V_{\text{eff}} = V_0 - V_{\text{appl}}$ , where  $V_0$  is the voltage when  $J_{\text{ph}}$  is 0, and  $V_{\text{appl}}$  is the applied bias voltage, and  $J_{\text{sat}}$  is representative of the saturation current.<sup>[18]</sup> The  $P(E, T)$  is expressed as  $P(E, T) = J_{\text{ph}}/J_{\text{sat}}$ . The  $P(E, T)$ s of **P1**, **P7**, and **P9** modified devices are 99.28%, 98.67% and 99.45%, respectively, which are equal or higher than that of PDINO (98.66%), indicating the efficient charge dissociation in the polycarbolong modified devices. Details are shown in Table S4. In addition, the charge recombination dynamics of different ETL-based OSC devices were investigated. As shown in Figure S178c, the slope

values for PDINO, **P1**, **P7**, and **P9**-based devices are 1.212, 1.114, 1.165, and 1.058  $kT/q$ , respectively,<sup>[19]</sup> suggesting that weak trap-assisted recombination exists in these devices. Meanwhile, the bimolecular recombination can be also characterized via the law  $J_{sc} \propto P_{light}^\alpha$ , where the index  $\alpha$  indicates the degree of bimolecular recombination in the device.<sup>[20]</sup> As shown in Figure S180, the  $\alpha$  values for **P1**, **P7**, and **P9**-based devices are 0.998, 0.995, and 0.999, respectively, suggesting that the bimolecular recombination are very weak in these devices, and are even lower than that in the PDINO modified device ( $\alpha = 0.985$ ).

**Table 2.** Photovoltaic parameters of PM6:EH-HD-4F-based OSCs with different ETLs.

ETLs	$V_{oc}$ [V]	$J_{sc}$ [mA cm <sup>-2</sup> ]	FF [%]	PCE [%]	$J_{cal}^{[b]}$ [mA cm <sup>-2</sup> ]
PDINO	0.83	27.47	77.16	17.62(17.54±0.12) <sup>[a]</sup>	26.12
<b>P1</b>	0.84	27.38	78.51	18.09 (18.04±0.05)	26.17
<b>P7</b>	0.83	27.38	76.91	17.69 (17.47±0.20)	26.19
<b>P9</b>	0.84	27.40	79.43	18.28 (18.24±0.04)	26.27

[a] Average value  $\pm$  standard deviation was obtained from 20 independent devices. [b]  $J_{sc}$  values were calculated from EQE curves.

Moreover, transient photocurrent measurements (TPC) were employed to investigate the charge extraction times.<sup>[21]</sup> As shown in Figure S178d, the charge extraction times of the **P1**, **P7**, and **P9** modified devices were fitted and found to be 0.647, 0.869 and 0.526  $\mu$ s, respectively, shorter than that in the PDINO-based device (1.059  $\mu$ s), indicating that the polycarbonyl modified devices could effectively facilitate charge carrier extraction. This may be partly due to their higher electron mobility ( $1.85 \times 10^{-3}$ ,  $1.78 \times 10^{-3}$ , and  $2.07 \times 10^{-3}$  cm<sup>2</sup>V<sup>-1</sup>S<sup>-1</sup>, respectively) in comparison with that of the PDINO modified device ( $8.58 \times 10^{-4}$  cm<sup>2</sup>V<sup>-1</sup>S<sup>-1</sup>), measured by space-charge-limited current (SCLC) as shown in Figure S181. Moreover, these polycarbonyl based devices also exhibit good stability (Figure S182). These results demonstrate that polycarbonyl can be used as efficient ETLs to increase the performance of OSCs.

## Conclusion

In summary, a  $d_{\pi}$ - $p_{\pi}$  conjugated strong acceptor building block with di-metallaaromatic structure was designed and synthesized, featuring a low-lying LUMO energy level. To insert this electron-deficient building block into conjugated polymer scaffolds, a double-monomer polymerization methodology was developed, resulting in a series of n-type polycarbonyls. This synthetic strategy enjoys the advantages of flexible selection of spacers, short synthetic procedures, good functional-group tolerance and high efficiency. The facile route can not only enrich the polymer structures but also tune the polymer properties, thereby broadening their application scopes. Some of them for example, exhibit broad and strong absorption, even in the NIR region.

Moreover, they have been shown to be promising candidates as electron transport layers in organic solar cells, boosting device performance. Specifically, the champion PCE based on **P9** was enhanced to 18.28%. Other properties and applications of such unique conjugated polymer systems are under further study.

## Acknowledgements

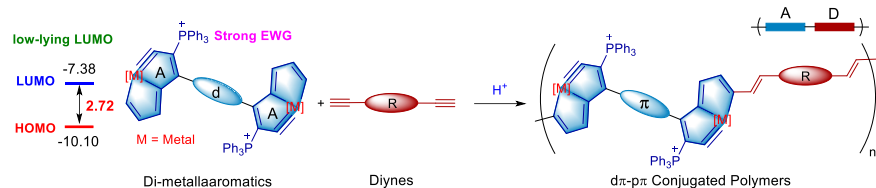
This research was supported by the National Natural Science Foundation of China (nos. 21931002, 92156021, and 21971216), Shenzhen Science and Technology Innovation Committee (JCYJ20200109140812302), Guangdong Provincial Key Laboratory of Catalysis (2020B121201002), Guangdong Grants (2021ZT09C064), and Project funded by China Postdoctoral Science Foundation (no. 2021M701567). The authors also thank financial support for Outstanding Talents Training Fund in Shenzhen and SUSTech Presidential Postdoctoral Fellowship.

**Keywords:** Electron-Deficient Building Blocks • Metallopolymers • Acceptor • Organic Solar Cells • n-Type Polymers

- [1] a) Z. Zhang, W. Wang, Y. Jiang, Y.-X. Wang, Y. Wu, J.-C. Lai, S. Niu, C. Xu, C.-C. Shih, C. Wang, H. Yan, L. Galuska, N. Prine, H.-C. Wu, D. Zhong, G. Chen, N. Matsuhisa, Y. Zheng, Z. Yu, Y. Wang, R. Dauskardt, X. Gu, J. B. H. Tok, Z. Bao, *Nature* **2022**, *603*, 624-630. b) H. Tang, Y. Liang, C. Liu, Z. Hu, Y. Deng, H. Guo, Z. Yu, A. Song, H. Zhao, D. Zhao, Y. Zhang, X. Guo, J. Pei, Y. Ma, Y. Cao, F. Huang, *Nature* **2022**, *611*, 271-277. c) X. Strakosas, H. Biesmans, T. Abrahamsson, K. Hellman, M. S. Ejneby, M. J. Donahue, P. Ekström, F. Ek, M. Savvakis, M. Hjort, D. Bliman, M. Linares, C. Lindholm, E. Stavrinidou, J. Y. Gerasimov, D. T. Simon, R. Olsson, M. Berggren, *Science* **2023**, *379*, 795-802. d) L. Meng, Y. Zhang, X. Wan1, C. Li, X. Zhang, Y. Wang, X. Ke, Z. Xiao, L. Ding, R. Xia, H.-L. Yip, Y. Cao, Y. Chen, *Science* **2019**, *361*, 1094-1098.
- [2] a) L. R. MacFarlane, H. Shaikh, J. D. Garcia-Hernandez, M. Vespa, T. Fukui, I. Manners, *Nat. Rev. Mater.* **2020**, *6*, 7-26. b) T. M. Swager, *Macromolecules* **2017**, *50*, 4867-4886. c) G. Zhang, F. R. Lin, F. Qi, T. Heumüller, A. Distler, H.-J. Egelhaaf, N. Li, P. C. Y. Chow, C. J. Brabec, A. K. Y. Jen, H.-L. Yip, *Chem. Rev.* **2022**, *122*, 14180-14274. d) A. K. Cheetham, R. Seshadri, F. Wudl, *Nat. Synth.* **2022**, *1*, 514-520.
- [3] a) Y. Liu, J. W. Y. Lam, B. Z. Tang, *Nat. Sci. Rev.* **2015**, *2*, 493-509. b) B. R. Boswell, C. M. F. Mansson, J. M. Cox, Z. Jin, J. A. H. Romaniuk, K. P. Lindquist, L. Cegelski, Y. Xia, S. A. Lopez, N. Z. Burns, *Nat. Chem.* **2021**, *13*, 41-46. c) X. Guo, A. Facchetti, *Nat. Mater.* **2020**, *19*, 922-928.
- [4] a) J. Chen, W. Huang, D. Zheng, Z. Xie, X. Zhuang, D. Zhao, Y. Chen, N. Su, H. Chen, R. M. Pankow, Z. Gao, J. Yu, X. Guo, Y. Cheng, J. Strzalka, X. Yu, T. J. Marks, A. Facchetti, *Nat. Mater.* **2022**, *21*, 564-571. b) H. Sun, X. Guo, A. Facchetti, *Chem* **2020**, *6*, 1310-1326. c) C.-Y. Yang, M.-A. Stoeckel, T.-P. Ruoko, H.-Y. Wu, X. Liu, N. B. Kolhe, Z. Wu, Y. Puttisong, C. Musumeci, M. Massetti, H. Sun, K. Xu, D. Tu, W. M. Chen, H. Y. Woo, M. Fahlman, S. A. Jenekhe, M. Berggren, S. Fabiano, *Nat. Commun.* **2021**, *12*, 2354.
- [5] a) H. Usta, A. Facchetti, T. J. Marks, *Acc. Chem. Res.* **2011**, *44*, 501-510. b) J. Chen, Y. Chen, L.-W. Feng, C. Gu, G. Li, N. Su, G. Wang, S.

- M. Swick, W. Huang, X. Guo, A. Facchetti, T. J. Marks, *EnergyChem* **2020**, *2*, 100042.
- [6] Z. Wu, C. Sun, S. Dong, X.-F. Jiang, S. Wu, H. Wu, H.-L. Yip, F. Huang, Y. Cao, *J. Am. Chem. Soc.* **2016**, *138*, 2004-2013.
- [7] Z. Chen, J. Li, J. Wang, K. Yang, J. Zhang, Y. Wang, K. Feng, B. Li, Z. Wei, X. Guo, *Angew. Chem. Int. Ed.* **2022**, *61*, e202205315.
- [8] K. Feng, H. Guo, H. Sun, X. Guo, *Acc. Chem. Res.* **2021**, *54*, 3804-3817.
- [9] a) R. Zhao, J. Liu, L. Wang, *Acc. Chem. Res.* **2020**, *53*, 1557-1567. b) K. Feng, H. Guo, J. Wang, Y. Shi, Z. Wu, M. Su, X. Zhang, J. H. Son, H. Y. Woo, X. Guo, *J. Am. Chem. Soc.* **2021**, *143*, 1539-1552. c) H. Bronstein, C. B. Nielsen, B. C. Schroeder, I. McCulloch, *Nat. Rev. Chem.* **2020**, *4*, 66-77.
- [10] a) J. R. Reynolds, B. C. Thompson, T. A. Skotheim, *Conjugated Polymers: Properties, Processing, and Applications*, CRC press, **2019**. b) H. Yan, Z. Chen, Y. Zheng, C. Newman, J. R. Quinn, F. Dotz, M. Kastler, A. Facchetti, *Nature* **2009**, *457*, 679-686.
- [11] D. Meng, R. Zheng, Y. Zhao, E. Zhang, L. Dou, Y. Yang, *Adv. Mater.* **2022**, *34*, 2107330.
- [12] R. Misra, S. P. Bhattacharyya, *Intramolecular charge transfer: theory and applications*, John Wiley & Sons, **2018**.
- [13] S. Chen, L. Peng, Y. Liu, X. Gao, Y. Zhang, C. Tang, Z. Zhai, L. Yang, W. Wu, X. He, L. L. Liu, F. He, H. Xia, *Proc. Natl. Acad. Sci. U. S. A.* **2022**, *119*, e2203701119.
- [14] Deposition numbers 2247929 (**1a**) and 2247930 (**1c**) contain the supplementary crystallographic data for this paper. These data are provided free of charge by the joint Cambridge Crystallographic Data Centre and Fachinformationszentrum Karlsruhe Access Structures service.
- [15] Z.-G. Zhang, B. Qi, Z. Jin, D. Chi, Z. Qi, Y. Li, J. Wang, *Energy & Environ. Sci.* **2014**, *7*, 1966-1973.
- [16] S. Chen, L. Feng, T. Jia, J. Jing, Z. Hu, K. Zhang, F. Huang, *Sci. China Chem.* **2021**, *64*, 1192-1199.
- [17] a) A. K. K. Kyaw, D. H. Wang, V. Gupta, W. L. Leong, L. Ke, G. C. Bazan, A. J. Heeger, *ACS Nano* **2013**, *7*, 4569-4577. b) J.-L. Wu, F.-C. Chen, Y.-S. Hsiao, F.-C. Chien, P. Chen, C.-H. Kuo, M. H. Huang, C.-S. Hsu, *ACS Nano* **2011**, *5*, 959-967.
- [18] L. Lu, T. Xu, W. Chen, E. S. Landry, L. Yu, *Nat. Photonics* **2014**, *8*, 716-722.
- [19] L. J. A. Koster, V. D. Mihailetschi, R. Ramaker, P. W. M. Blom, *Appl. Phys. Lett.* **2005**, *86*, 123509.
- [20] P. Schilinsky, C. Waldauf, C. J. Brabec, *Appl. Phys. Lett.* **2002**, *81*, 3885-3887.
- [21] Z. Li, F. Gao, N. C. Greenham, C. R. McNeill, *Adv. Funct. Mater.* **2011**, *21*, 1419-1431.

## Table of Contents



We designed a di-metallaaromatic acceptor with strong electron-withdrawing ability, and introduced it to a series of d $\pi$ -p $\pi$  conjugated metallopolymers using a double-monomer polymerization methodology. These metallopolymers can be applied as electron transport layer materials of an organic solar cell, improving the power conversion efficiency considerably.